JETIR.ORG ISSN: 2349-5162 | ESTD Year : 2014 | Monthly Issue
JOURNAL OF EMERGING TECHNOLOGIES AND INNOVATIVE RESEARCH (JETIR)
An International Scholarly Open Access, Peer-reviewed, Refereed Journal

DESIGN AND DEVELOPMENT OF A SUB-ORBITAL PAYLOAD SOUNDING ROCKET USING OPENROCKET

Shashank Sharma1, Narendra Kumar2, Hari Om Singh3

Department of Aerospace Engineering, School of Engineering and Information Technology, IIMT UNIVERSITY, Meerut, Uttar Pradesh, India.

1. INTRODUCTION

Sounding rockets play an important role in aerospace research. They serve as affordable sub-orbital platforms that carry scientific instruments and payloads into the upper atmosphere. Unlike orbital launch vehicles, sub-orbital sounding rockets follow a parabolic path. They ascend to a target altitude and experience brief periods of microgravity, extreme acceleration, or unique atmospheric conditions before returning to Earth with controlled recovery systems. These missions are essential for gathering meteorological data, sensing the atmosphere, and testing sub-systems like Can-Sats or other specialized research modules in real flight conditions.

In order to design a stable sounding rocket, a multidisciplinary engineering approach must be employed to consider factors relating to structure aerodynamics, efficiency of propulsion system, ability for recovery and structural stability of the rocket itself. Important aerodynamic elements include the design of the nose cone (such as ogive or parabolic design), airframe (body tube), and the design of fins that will help control the rocket's movement within the atmosphere. As the pressure decreases rapidly, along with the intense mechanical vibration felt by the rocket while traveling sub-orbitally, the payload and structure of the rocket must be carefully examined.

Conventionally, the process of developing a rocket vehicle was fraught with the use of intricate mathematical equations, CFD solver or even expensive physical prototypes. Nevertheless, contemporary aerospace engineering negates all these challenges by using a reliable and accurate simulation software of aircraft flights. Open-Rocket is one such highly rated and free simulation software that allows engineers to develop their own rockets in totality. This software computes vital parameters, including apogee, maximum speed, structural mass and flight calibers.

Through the use of Open-Rocket, designers can virtually test the complete flight process, which includes optimizing the interior assembly space (for example the payload compartment and the engine compartment), checking the CG in relation to CP, and finally testing the release of the recovery mechanism. In this paper, the design and simulation process of a suborbital sounding rocket for carrying a payload will be discussed. The rocket design is optimized via virtual testing in Open-Rocket to successfully launch the required payload weight to the desired altitude.

2. LITERATURE REVIEW

Sub-orbital sounding rockets have a very complex and integrative multidisciplinary design which involves the integration of propulsion mechanics, weight and structure margining, aerodynamics, and recovery mechanisms. Sounding rockets have been playing a vital role for decades in bridging the gap between tests done at ground level and those done at full orbit insertion. In educational and academic aerospace programs, sounding rockets have been used extensively to launch scientific modules like Can-Sats or atmospheric sensors into the upper levels of the troposphere and stratosphere. One of the main criteria in university-level aerospace studies is designing a vehicle using single stage for launching the standard atmospheric payload, weighing around 150 grams, up to a certain altitude before triggering the recovery phase. The research work carried out by Campbell and Okutsu emphasizes that the perfect match of the thrust curve to the structural design is needed to predict the flight variables including velocity, flight time, and apogee.

First, the key factor in the construction of small rockets is the mathematical split between wet mass 1000 grams upon takeoff, including unspent propellant) and dry mass (667 grams after propellant burnout). This structure-related mass ratio governs the kinetic energy transfer at the burnout stage. From classical principles of flight dynamics, lighter structural elements minimize the effect of drag and contribute to higher velocities during the burnout. Nevertheless, payload-carrying rockets require high structural integrity to prevent dangerous aeroelastic instability during transition through zones of maximum aerodynamic pressure. It is known from literature that payload compartments, which accommodate, for instance, 150 grams payload modules, should be mounted as far forward as possible on the airframe to move the Center of Gravity (CG) forward relative to the Center of Pressure (CP).

A strictly empirical approach based on the physical modeling in modern engineering design is unprofitable economically and may pose danger to flights safety. Open-Rocket is one of the leading open-source software solutions for aerodynamic calculations and trajectory prediction. The external geometrical shape is analyzed (the nose cone profiles and fin set), the classical equations of motion are solved taking into account changes in the atmosphere. Open-Rocket uses Barrowman Equations to calculate the static stability, setting up the classic caliber rule, according to which the distance between CG and CP should be no less than (1.5 – 2 times) the body tube diameter. Data obtained during the simulation enables the designer to predict altitude-time trajectories and evaluate the impact of fuel mass reduction from the initial 1000 grams wet weight down to 667 grams dry weight.

Finally, the recovery process marks the last key step of the sounding rocket process. The typical approach to the problem of model rockets is extensively described in standard literature and implies the use of apogee-triggered parachute deployment through pressurization of the body tube by black powder or servo-mechanical actuators. However, the more sophisticated missions of atmospheric or meteorological research imply mid-flight double deployment or separation of the payload pre-apogee. Launching of the special 150 grams payload at the predetermined altitude (as the example of launching of the payload at the altitude of 450 m in case of 500 m rocket flight in this work) allows for accurate measurements without contamination by the aerodynamic wake of the vehicle itself or its exhaust plume. Simulation of this effect in Open-Rocket software becomes extremely important, as the sudden loss of airframe mass and geometry results in significant changes of the CG and descent speed that should be precisely calculated to avoid excessive speeds or deviations of trajectory. Finally, using Open-Rocket in designing such mid-flight 450 m deployment process becomes the example of optimization problem solution.

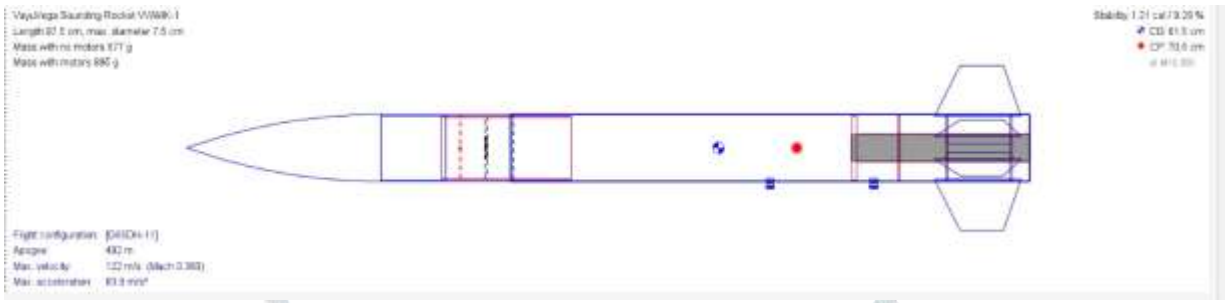

Figure.1 Schematic Diagram of Rocket

3. DESIGN METHODOLOGY

3.1 Structural layout and Material Specifications

The structural layout of the Vayu-Vega VVAMK-1 is designed to maximize the balance between aerodynamics, internal packaging, and structural strength when subjected to high levels of thrust. The vehicle features a single stage, modular airframe design.

Forebody Nose Cone Geometry: A tangent **Ogive profile** with a total axial length of 22.5 cm is selected to minimize drag in the subsonic and low-transonic regimes. It is manufactured using Acrylonitrile Butadiene Styrene (**ABS**) with a 100% infill density ($\rho = 1.05\ g/cm^3$), yielding a total component mass of 72.4 g.

Payload Bay Architecture: Positioned immediately aft of the nose cone, a 15 cm long Polyvinyl Chloride (**PVC**) compartment ($\rho = 1.39\ ^{g}_{cm^3}$) serves as the payload bay. It features an outer diameter (D_{out} = 7.5 cm and an inner diameter

(D_{in} = 7.1 cm), bringing its independent structural mass to 95.6 g. A 15 cm PLA tube coupler resides internally to join the airframe segments seamlessly.

Main Body Tube: The primary structural core is a 60 cm PVC fuselage segment sharing identical diameter constraints($D_{out} = 7.5\ cm, D_{in} = 7.1\ cm$). It possesses a component mass of 187 g and houses the recovery system, internal anchoring bulkheads, and the propulsion sub-assembly.

Internal Motor Mount & Alignment: To safely transfer thrust loads to the outer airframe, a 20 cm PVC inner tube$D_{out} = 3.1\ cm\ D_{in} = 2.9\ cm$, Mass = 26.2 g) is rigidized coaxially within the main body tube. This inner core is secured via **three 0.2 cm thick PLA centering rings** (Centering Rings 1, 2, and 3), each weighing 8.29 g with an outer
diameter of 7.2 cm and an inner diameter of 3.1 cm. An Engine Block (0.5 cm length) prevents forward structural slippage of the motor casing under peak acceleration.

3.2 Aerodynamic Stabilizing Surface Design

Passive aerodynamic stability is provided via a radially symmetric **4-fin empennage configuration** located at the extreme aft of the vehicle.

- **Fin Geometry:** The fins utilize a **trapezoidal profile**, which provides excellent structural stiffness and minimizes tip-vortex induced drag compared to delta or rectangular profiles.
- **Material Properties:** The entire 4-fin set is 3D-printed out of Polylactic Acid (**PLA**) at a 100% infill density$\rho = 1.25\ \frac{g}{cm_3}$).
- **Physical Dimensioning:** The total assembly mass of the fin set is 91.6 g, with each fin maintaining a rigid thickness of 0.3 cm to resist aerodynamic flutter during high V_{max} phases.

3.3 Propulsion & Ballistic Characteristics

The vehicle is propelled by a single commercial high-power solid rocket motor. The selection of the motor dictates the initial launch acceleration and optimal deployment sequencing.

Solid Rocket Motor Parameter Specification Value Motor Classification Code
G65DH-11
Total Impulse (I_s)
136 Ns
Maximum Thrust (F_{max})
88.7 N
Average Thrust (F_{avg})
69.6 N
Burn Time (T_b)
1.95 s
Total Motor Mass (M_m)
93 g
Physical Dimensions (Diameter / Length)
29 mm / 206 mm
Thrust-to-Weight Ratio
7.93:1

Table.1 Motor Specifications

The high thrust-to-weight ratio ensures that the rocket accelerates rapidly down the rail, achieving a **velocity off the pad of 11.3 m/s**. This rapid exit velocity guarantees that the aerodynamic fins achieve immediate control authority, heavily suppressing any off-nominal weathercocking from crosswinds.

3.4 Static Mass Properties & Barrowman Stability

Static stability is calculated analytically using the spatial relationship between the vehicle's Center of Gravity (CG) and Center of Pressure (CP) relative to the forwardmost tip of the nose cone. The wet mass of the completed vehicle assembly stands at **895 g**.

- **Center of Gravity (X_{CG}):** Located at **61.5 cm** from the nose tip.
- **Center of Pressure (X_{CP}):** Located at **70.6 cm** from the nose tip.
- **Static Margin Calculation:** $\frac{(XCP-XCG)}{D_{out}} = \frac{70.6\ cm - 61.5\ cm}{7.5}$

- **Static Margin (Percentage of Length): 9.29%**

A static stability margin of 1.21 calibers safely positions the vehicle within the ideal stability window(1.0 cal ≤ margin ≤ 2.0 cal). This prevents both unstable, erratic flight paths(≤ 1.0 cal) and hyper-sensitive over-stable conditions (≥ 2.0 cal).

3.4 Recovery Subsystem & Payload Integration

The internal vehicle volume is split to safely accommodate a functional atmospheric telemetry payload and a deployable recovery system.

- **Payload Module Integration:** The payload compartment houses a standardized **150 g Can-Sat Module** ($D_{out} = 7.1\ c$), isolated from the recovery deployment forces within its own PVC bay.
- **Kinetic Shock Absorption:** A 60 cm braided nylon shock cord (3 mm / 1/8 in diameter, linear density of 3.5 g/m) acts as the elastic tether between the split airframe components, mitigating the peak opening shock of the deceleration system. The total cord mass is 2.1 g.
- **Deceleration Canopy:** A **60 cm diameter Ripstop Nylon parachute**, (67.5 $\frac{g}{cm_2}$, component mass of 25.4 g) provides drag area maximization for descent. It utilizes 6 independent 60 cm round elastic shroud lines (2 mm diameter, 1.8 g/m linear density) to securely anchor the canopy to the harness loop.
- **Launch Rail Interface:** Mechanical alignment along the launch rail is maintained by two low-drag Delrin rail buttons (Mass = 0.827 g each) affixed directly to the PVC airframe.

3.5 Flight Kinematics & Trajectory Timeline

Based on mathematical and programmatic design tracking, the operational flight path profile follows a rigorous state sequence:

Boost Phase: Motor ignition supplies thrust over a 1.95 s window, forcing the vehicle up to a **Maximum Velocity (*Vmax*122 m/s**.

Coast Phase: Following motor burnout at 1.95 s, the rocket converts its kinetic energy into potential altitude, coasting for an additional 7.74 s.

Apogee Event: The vehicle peaks at a maximum **Apogee Altitude of 492 m** at exactly t = 9.69 sec.

Recovery Ejection Sequencing: An optimal motor delay of **7.71 s** executes post-burnout. Ejection occurs at a safe velocity of **23.5 m/s** to preserve structural canopy integrity.

Terminal Descent Phase: The deployed parachute reduces descent velocity to a stable **Terminal Landing Velocity of 7.76 m/s**, bringing the total mission flight time to **66.6 s.**



Figure.2 3-D Figure of Sounding Rocket

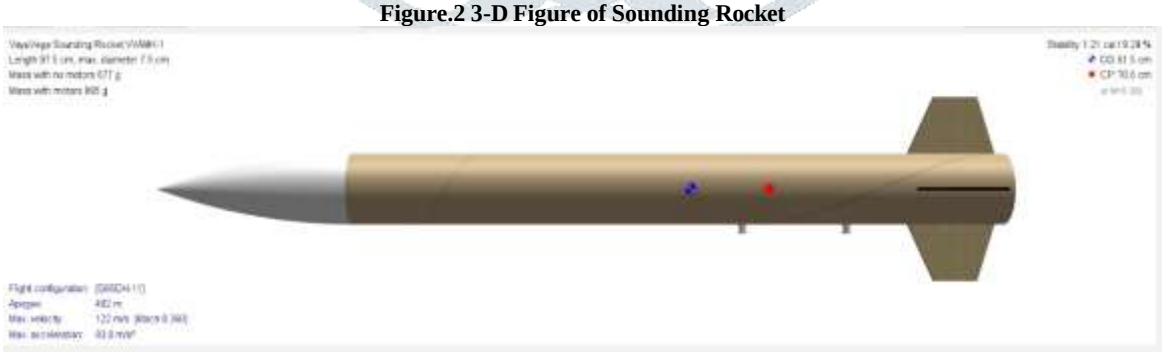

Figure.3 CAD Model for Sounding Rocket

4. COMPONENTS OF MODEL ROCKET

1. NOSE CONE

The nose cone is located at the most extreme front of the rocket and plays an important role in terms of aerodynamics in managing air flow around the rocket body tube by directing airflow correctly to reduce drag. There is a difference in the aerodynamic resistance that each type of nose cone geometry produces; hence, a particular nose cone is chosen based on aesthetics and the drag coefficient (Cd) associated with it. In terms of its physical properties, it can be made of non-metallic light materials such as 3D-printed ABS plastic material with full density (1.05 g/cm3) having an aerodynamic design such as Ogive shape. Apart from being used for aerodynamics purposes, the nose cone interior space can be utilized in adjusting the center of gravity (CG) of the

rocket if it needs to be balanced for stable flight.



Figure.4 Nose Cone

2. PAYLOAD BAY

The payload bay is a specialized modular segment of the aircraft built for containing and isolating sensitive electronics, scientific instruments, or cargo. Built from the same material as the airframe (for example, PVC pipes), it acts as a barrier to separate the sensitive tracking payloads and altimeters from the hot gases released by the ejection charge during recovery. To ensure this segment does not disrupt the streamlined shape of the rocket in any way, an internal Tube Coupler (usually made of PLA using 3D printing) is used to make the connection between body tubes internally seamless and therefore remove all external irregularities that might introduce parasitic drag. In addition, since the payload contained within the payload bay introduces local mass, its positioning at the front of the rocket becomes an important design parameter which moves the CG of the rocket forward, allowing the engineers to keep a stable flight margin with respect to CP.

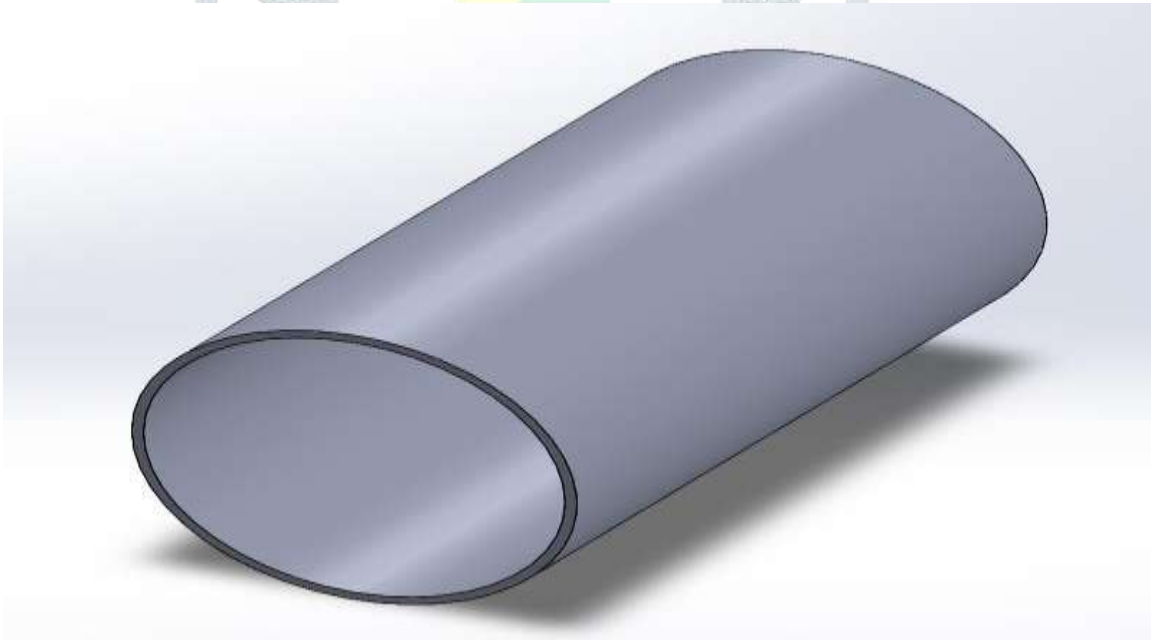

Figure. 5 Payload Bay

3. BOOSTER SECTION

Body tube is used as the main structural fuselage or airframe of the model rocket, providing a relatively light structure containing all the inner modules. In terms of meeting the safety standards, it is important that the airframe should be made of non-metallic materials, including reliable plastic pipes made of Polyvinyl Chloride (PVC) (for example, with the inner diameter of 7.1 cm and the outer diameter of 7.5 cm). For those cases when there is a need to have several modular sections, including having a separate Payload Bay to carry different sensors or cargo, it becomes necessary to have an inner element called a Tube Coupler. The tube coupler is usually made of polymer materials such as PLA.

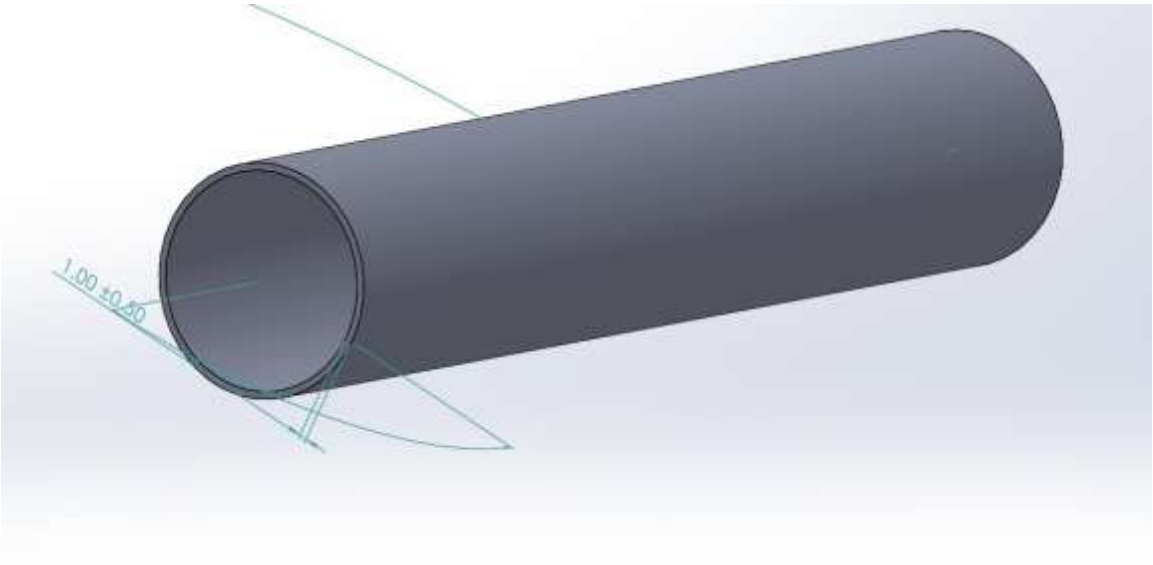

Figure. 6 Booster Section

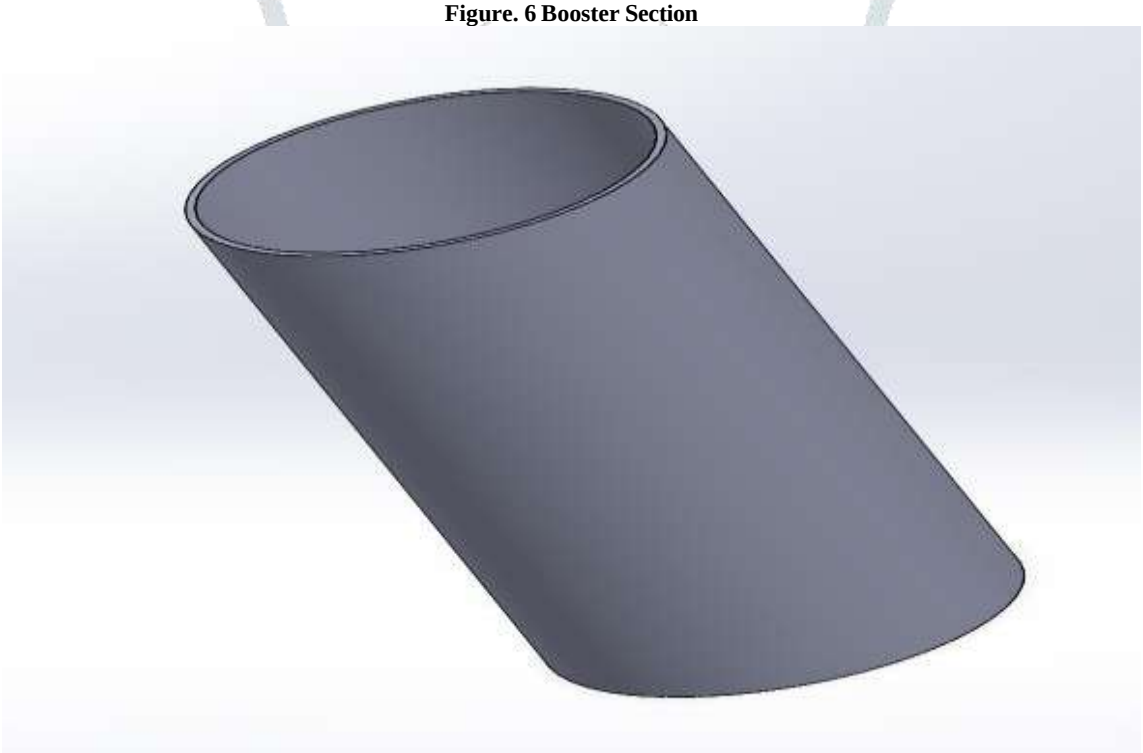

Figure.7 Coupler

4. FINS (TRAPEZOIDAL)

The fins are aerodynamically stabilizing structures that have been attached to the outside surface of the body tube in order to ensure aerodynamic stability through control of the Center of Pressure (CP). To avoid any structural failures from occurring due to high levels of aerodynamic forces, the type of material used for the fins should be chosen very carefully, together with the correct wood grain orientation in cases where wood is employed. For example, in cases where light weight balsa wood is used, the wood grain should be oriented parallel to the leading edge instead of the body tube because wrong orientation would lead to the fin shearing and breaking during flight.

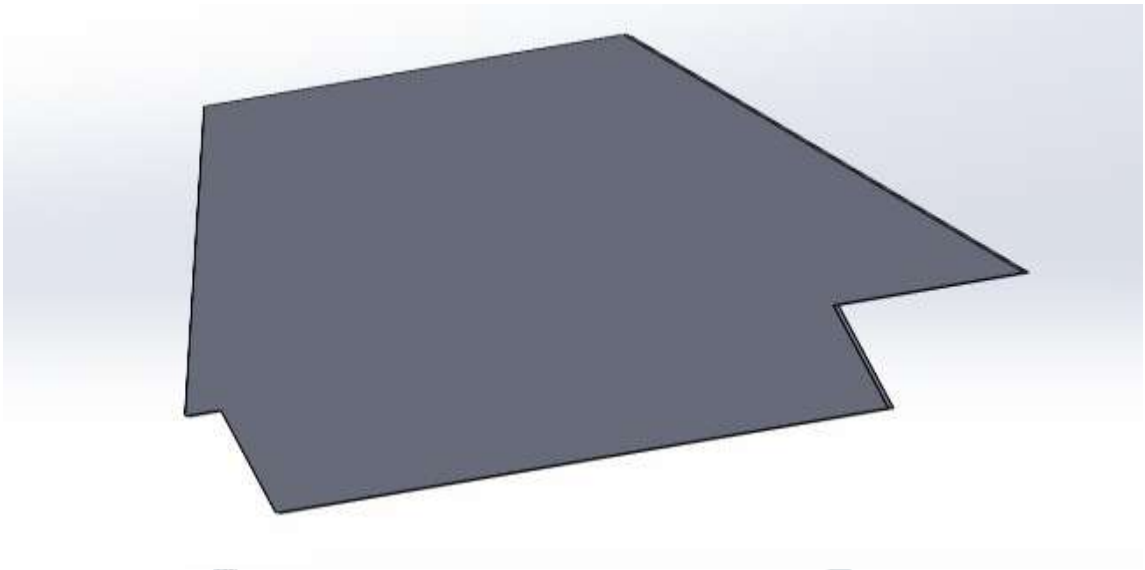

Figure.8 Trapezoidal Fin

5. INNER MOUNT (PROPULSION SYSTEM)

The propulsion system generates the required thrust for the acceleration of the rocket and determines the maximum altitude, the trajectory followed, and the burn characteristics of the vehicle. The propulsion system uses solid-fuel commercial-certified Rocket Motors (G65DH composite motor with average thrust 69.6 N/s and total impulse of 136 N/s. The rocket motor is housed in a smaller Inner Tube located at the bottom of the fuselage. In order to properly secure this inner tube and ensure it is perfectly aligned along the longitudinal axis of the rocket, two rigid discs called Centering Rings (machined or 3D-printed using 100% PLA infill) are fixed in between the two tubes.

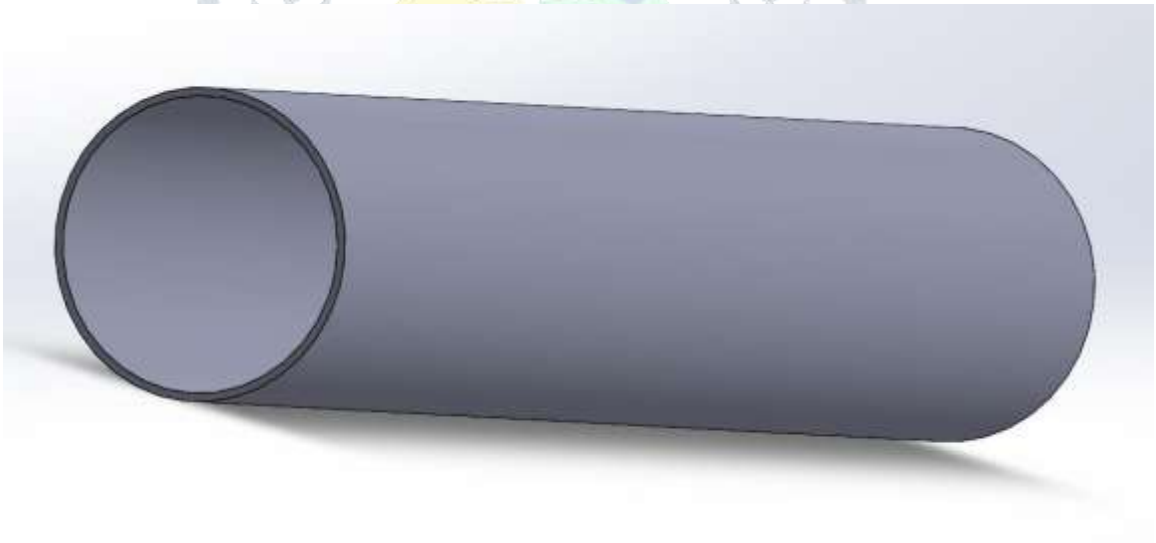

Figure.9 Inner Mount

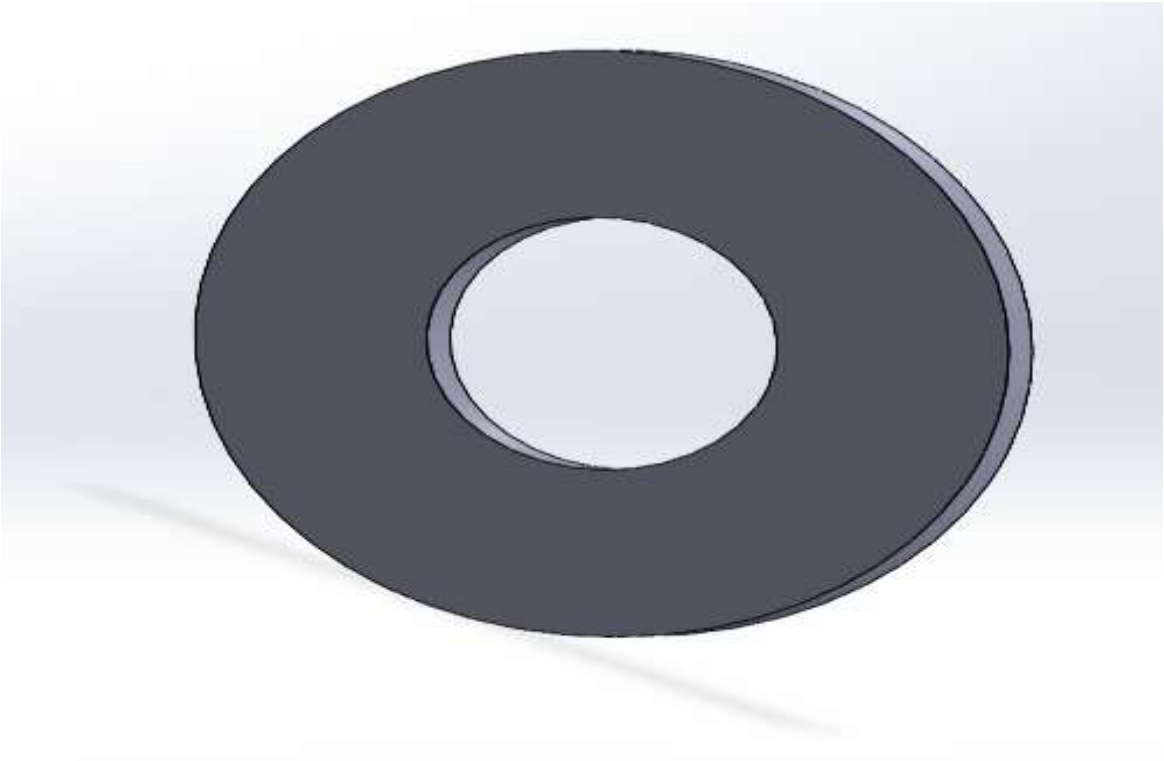

Figure. 10 Centering Ring

6. RECOVERY SYSTEM

The recovery mechanism safely slows down the rocket on its descent to guarantee that it lands without any damage and can thus be reused again in subsequent flights. This is achieved by utilizing a very strong yet light fabric like Ripstop Nylon ($67\ g/cm^2$) attached to elastic lines to generate maximum drag force and achieve a safe landing speed. This deployment canopy is then mounted to the airframe using a Shock Cord which is very strong and is constructed out of braided nylon. Since the deployment of the recovery system uses a high-power black powder or composite motor ejection charge, the shock cord mount needs to be heavily reinforced with multiple layers of adhesives and paper to withstand the intense mechanical stress at an instant. Also, a flame-retardant or fireproof wadding must be placed in the body tube below the parachute to act as a barrier against the hot gases.

5. OPEN ROCKET FLIGHT SIMULATION

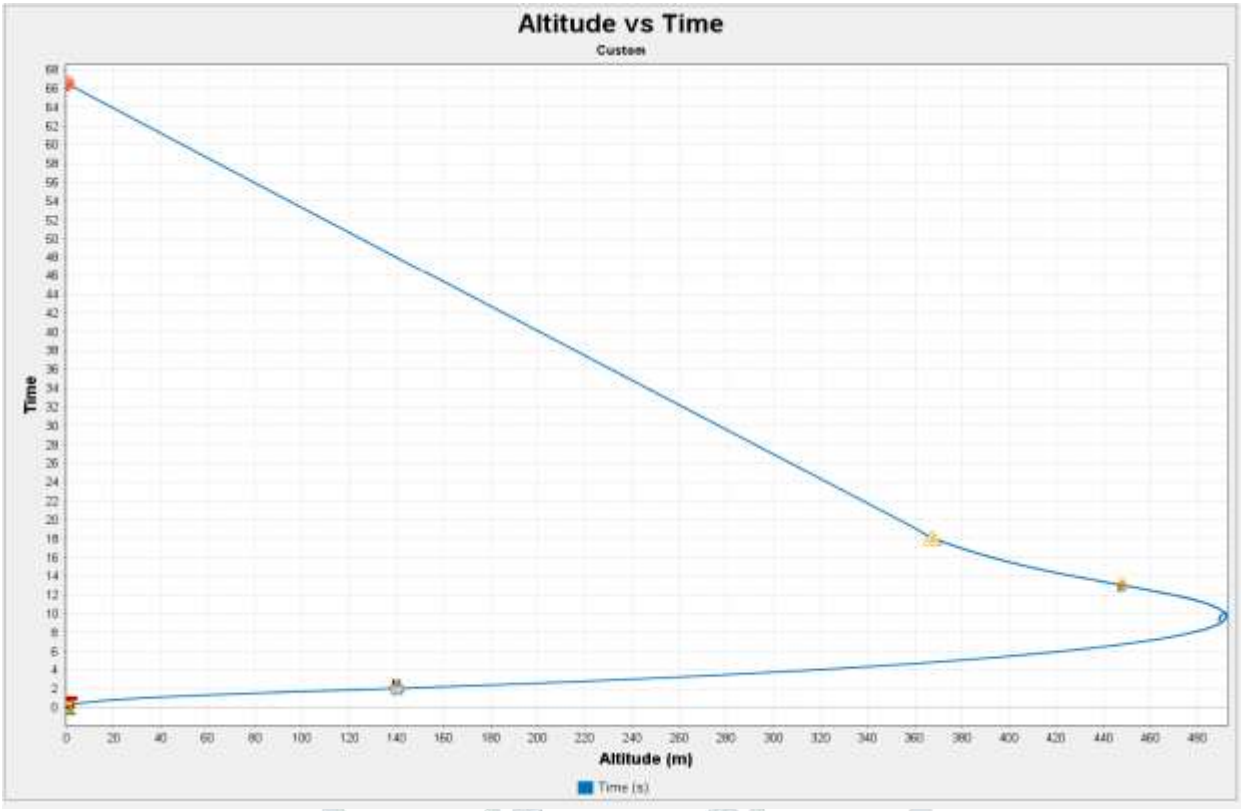

Figure. 11 Altitude vs Time

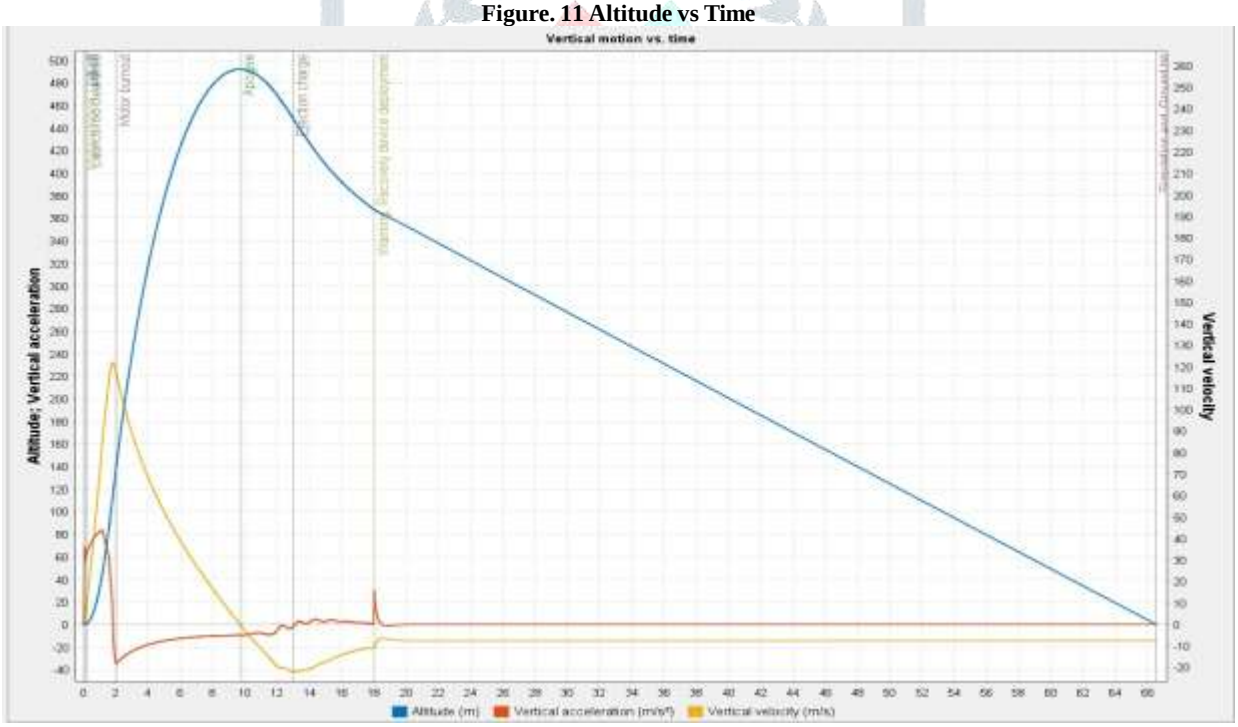

Figure.12 Time vs Vertical Acceleration and Vertical Velocity

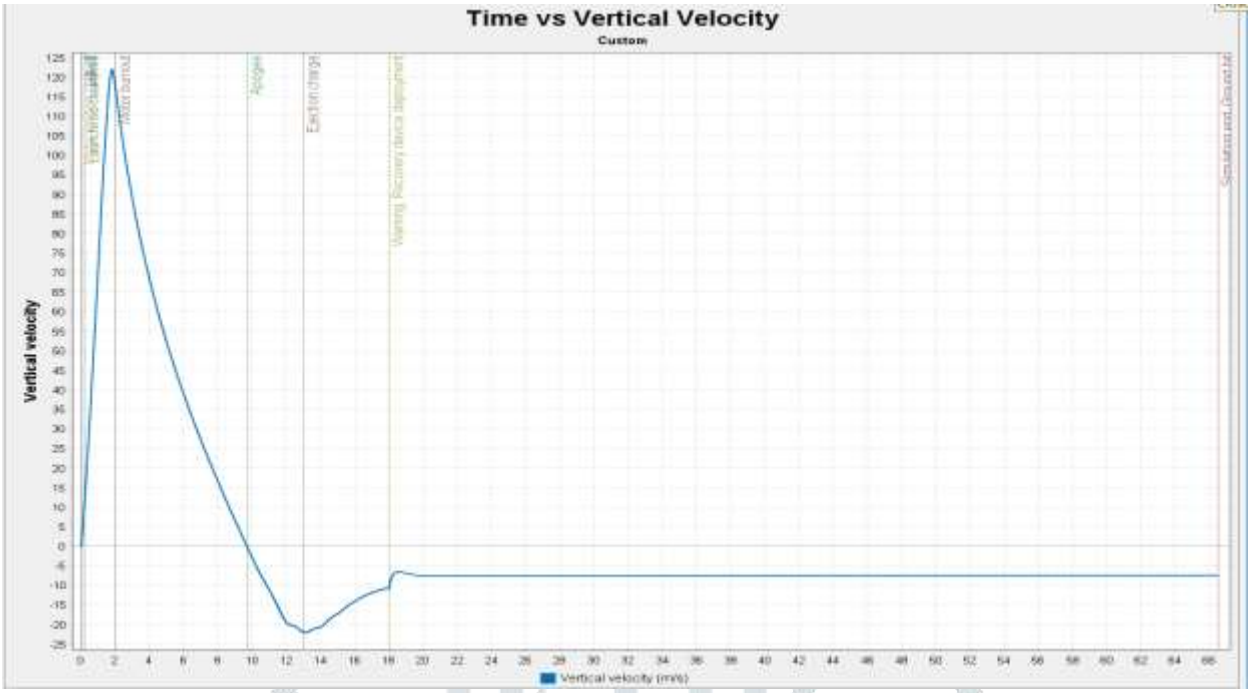

Figure.13 Time vs Vertical Velocity

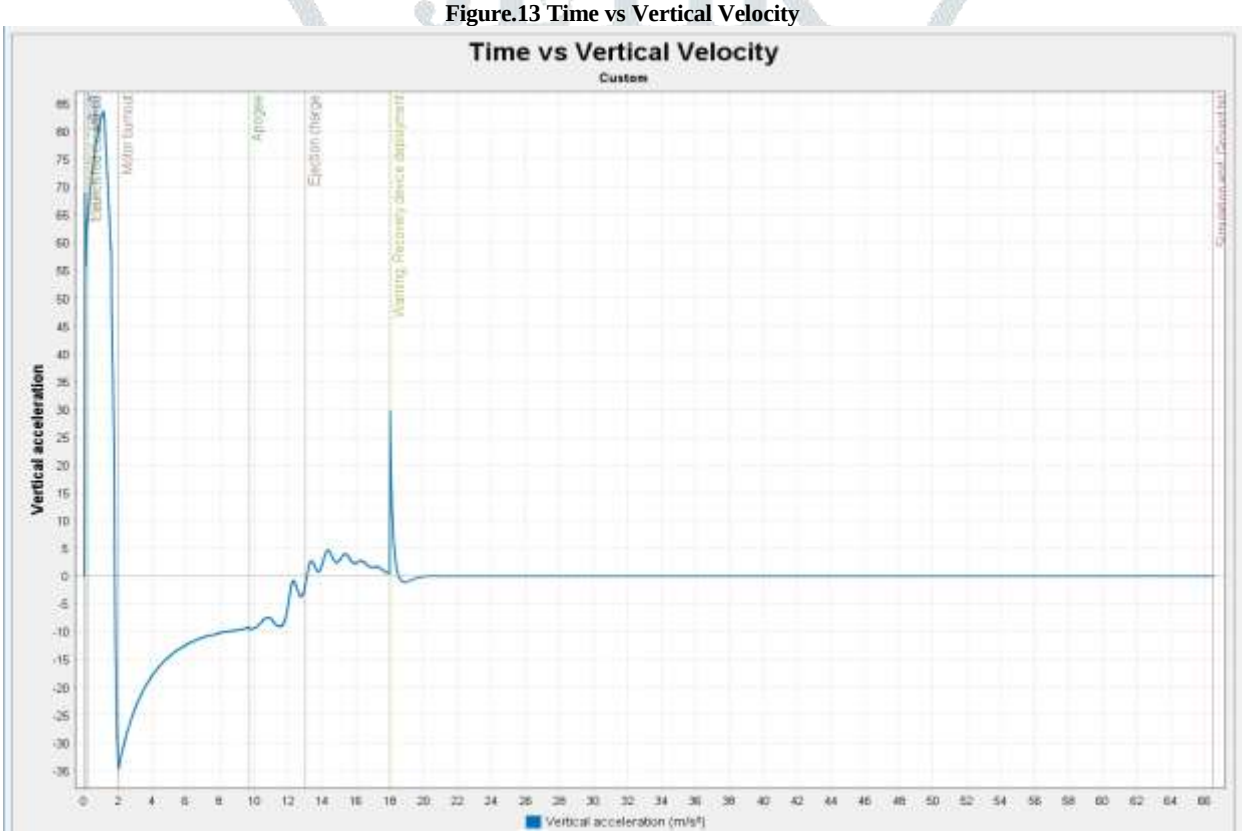

Figure. 14 Time vs Vertical acceleration

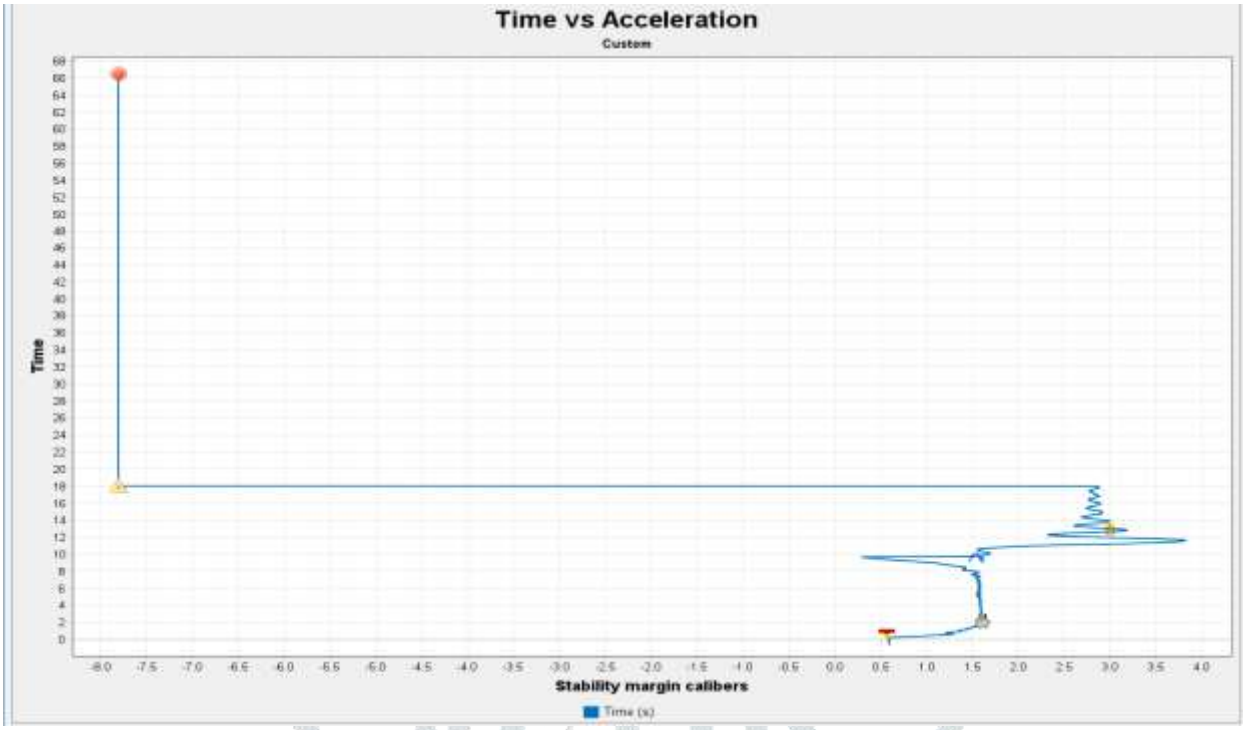

Figure. 15 Time vs Stability Margin

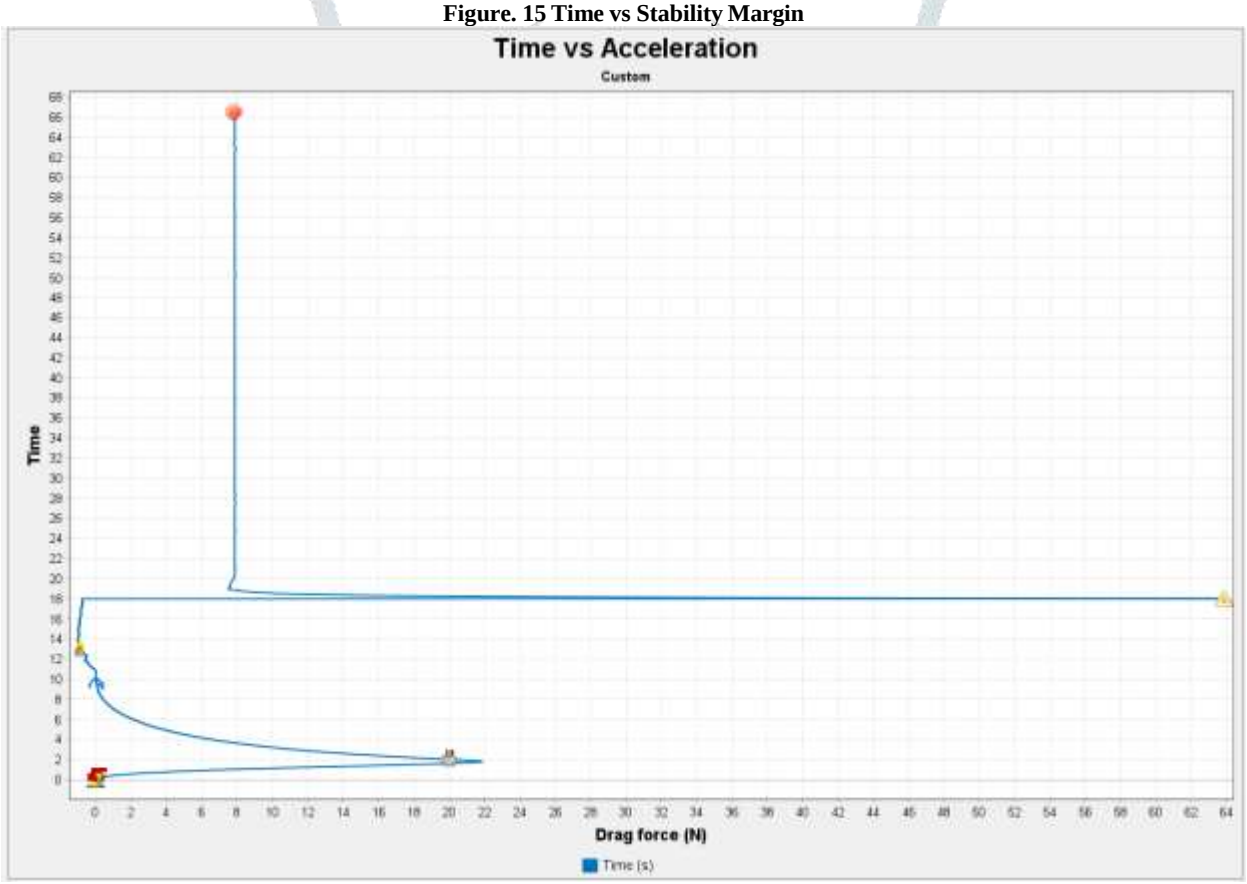

Figure.16 Time vs Drag Force

RESULTS

Integrated analysis of launch vehicle telemetry graph data alongside corresponding design data has yielded insight into the dynamically rich nature of a flight profile where the criticality of the payload bay in determining the overall stability and kinematics became clear. With the help of an anchoring system consisting of the rocket's PVC-body tube-airframe and an internal PLA-tube-coupler, the model rocket was able to maintain a static stability margin of roughly 0.55 calibers when launched using a standard solid-propellant-composite-rocket-motor. During the brief but powerful powered ascent period, the vehicle experiences rapid acceleration, reaching a peak vertical acceleration of roughly 83 m/s^2, while also subjecting itself to large amounts of aerodynamic drag due to the very high velocities reached. As expected for a solid-fueled vehicle, the engine quickly burned out resulting in both a reduction

in forces experienced and a sharp increase in altitude achieved. Specifically, we see from our telemetry data that at precisely t=2.0 seconds, the vehicle achieves a peak vertical velocity of 122 m which corresponds to the end of powered ascent and ignition of the rocket engine. At this point, the vehicle is experiencing its maximum amount of atmospheric resistance with an associated peak force magnitude of about 22 Newtons. Throughout the entire powered phase, as the rocket consumed more and more solid propellant at its posterior location, the Center of Gravity (COG) would migrate forward, closer to the front-nose-cone and payload-bay locations. This resulted in a growing separation between the COG and the Center of Pressure (COP) and led to a smooth transition in static stability margins from 0.55 calibers all the way up to 1.6 calibers at burn out. With the completion of motor burnout at t = 2 sec, the rocket entered a coasting stage with deceleration due to gravity and residual drag force acting on it. At motor burnout, the acceleration of the rocket experienced a sudden fall to reach a minimum value of about 34 m/s after which it began to stabilize. As the rocket kept converting its kinetic energy into potential energy, its velocity continued to decrease until it reached 0 m/s} at t = 9.8 sec, resulting in the maximum apogee of 492 meters of the rocket. During the coast phase leading up to apogee (from t = 10 sec to t = 13 sec), there were some transient oscillations of the static stability margin in the range of 2.75 to

3.80 calibers, caused by changing angles of attack as the rocket lost the last of its velocity. Structural strength of the forward payload bay became crucial at this stage since it physically protected onboard instrumentation from any vibrations and environmental effects. The rocket's descent and recovery phase commenced shortly thereafter. At t=13.1s, the internal delay for the rocket's motor had concluded, triggering the ejection charge which activated the recovery system (drag fluctuation). At t=18.0s the main recovery

device (the rocket) fully inflated creating a mechanical shock to the entire structure with a massive amount of drag at this point, which resulted in an instantaneous increase of deceleration drag of magnitude 64N. This large surge of energy was efficiently dissipated by transferring stress from ripstop nylon canopy along the braided nylon shock cord assembly into the reinforcement airframe. Simultaneously, when the parachute was deployed well above the body of the rocket, all the aerodynamics flipped on their head such that the center of drag moved far forward of the CG resulting in a constant negative value (-7.80 calibers) of stability margin which has mathematical properties consistent with a stable suspension where the rocket descends nose up. This attitude kept the payload bay free of structural loads due to descent while the parachute applied a constant level of drag (~8N). As the parachute increased its surface area and slowed down more it started to reach a terminal velocity of ~-7.5m/s prior to final landing at t=66.5s.

CONCLUSIONS AND FUTURE WORK

The success of this investigation was validated by the evaluation of the aerodynamic performance, structural integrity, and stability of a modular model rocket equipped with a payload bay in isolation. A non-metallic PVC airframe, and an internal tube coupler made of a plastic material PLA ensured sufficient structural integrity capable of sustaining the peak flight loads while avoiding any surface discontinuities and drag. Kinematic analysis showed that the maximum vertical speed of 122 meters was attained during the motor burnout at t = 2.0 sec and the apogee height was 492 metre. The correct position of the payload bay allowed for optimal balancing of the vehicle mass, thus widening the static stability margin up from 0.55 calibers initially to 1.62 calibers after the motor burnout in order to prevent tumbling under aerodynamic influence. Moreover, the payload bay provided additional structural protection of the onboard instrumentation from the hot gasses of the ejection mechanism and the shock of 64 N/s deployment forces. Consequently, a safe descent speed of 7.5 m/s and recovery at t = 66.5 sec were attained. Aerodynamic Efficiency Optimization: Future iterations can explore advanced nose cone geometries (parabolic/von Kármán) with empirically determined drag coefficients (Cd). Upgrading core airframe construction from PVC piping to advanced composites (carbon fiber/lightweight fiberglass) will dramatically reduce dry mass and improve thrust-to-weight ratio. Stability Augmentation System Implementation: Incorporating active stabilization technologies (automated fin control surfaces/cold-gas TVM module) could eliminate transient stability oscillations experienced near apogee while maintaining static stability margins. Dual-Deployment Recovery Sequence Implementation: Employing staged parachute deployment (low-drag "drogue" at apogee/primary ripstop nylon canopy at lower set-altitude) will limit wind drift effects during descent and ensure vehicle remains localized to defined landing area.

REFERENCES

1. *VayuVega Design Configuration*, Document Report, 2026.

2. T. A. Campbell Jr. and M. Okutsu, "Model Rocket Project for Aerospace Engineering Course: Trajectory Simulation and Propellant Analysis," Department of Mechanical Engineering, The Catholic University of America, Washington D.C., USA, Tech. Rep., 2016.

3. D. M. Ponder, *Designing Your Own Model Rocket*, Ohio State University Extension, 2013.

4. R. H. Burth *et al.*, *NASA Sounding Rockets User Handbook*, Peraton Inc., NASA Wallops Flight Facility, Wallops Island, VA, Tech. Pub. NASA/TP-20230006855, May 2023.

5. S. Testé *et al.*, "Team 124 Project Technical Report for the 2018 IREC/SAC," AstroJays Technical Report, The Johns Hopkins University, Baltimore, MD, Tech. Rep., 2018.

6. T. Van Milligan, "What parts can be made by 3D printing?," *Peak of Flight Newsletter*, no. 482, Nov. 13, 2018.

7. S. Thorat, N. Laddha, and N. Mehendale, "Design and development of a model rocket with recovery system and thrust vectoring for enhanced performance and stability," *SSRN Electronic Journal*, SSRN paper 5012956, [n.d.].

8. *Modular Model Rocket for A/B/C Motors Instruction Guide*, [n.a.], [n.d.].

9. *Designing a Model Rocket with OpenRocket: This Document Adheres to the UKROC 2026 Rules Only*, [n.a.], [n.d.].

10. "Model rocket parameters," Perplexity AI compilation report, [n.d.].

11. National Aeronautics and Space Administration, *NASA Sounding Rockets User Handbook*, Sounding Rockets Program Office, Sub-orbital and Special Orbital Projects Directorate, Wallops Flight Facility, Jul. 2015.

12. H. Gamal and M. G. Abdelhady, "Design and manufacture of a sounding rocket: Propulsion, aerodynamics and control," Graduation Project, Aerospace Engineering Department, Faculty of Engineering, Cairo University, Jul. 2016.

13. G. D. J. Harper, *50 Model Rocket Projects for the Evil Genius*. New York, NY, USA: McGraw-Hill, 2007.

14. N. Jamal, T. S. Bangari, N. Singh, and V. Babu, "Rocket flight simulation using AI/ML," *JAAFR Journal of Advance and Future Research*, vol. 3, no. 12, Dec. 2025.

